Rev. Mexicana Astron. Astrof., **23**, 203-215 (1992)

MOLECULAR OPACITIES IN M-STAR ATMOSPHERES

F. Allard,
Department of Physics
University of Montreal

M. Scholz and R. Wehrse
Institut f. Theoret. Astrophysik
Universität Heidelberg

RESUMEN. Se revisan brevemente las propiedades de las atmósferas de las gigantes y enanas M, y se decriben los problemas de los modelos. Demostramos, por medio de cálculos recientes de atmósferas de enanas, que las moléculas son de importancia clave en la ecuación de estado y que cuya absorción determina en la mayoría de los casos la pendiente del espectro. Una comparación entre los espectros calculados y observados del sistema de la enana M Gliese 866 demuestra las limitaciones del modelo que se emplea y la necesidad de mejores datos sobre el equilibrio y las opacidades moleculares.

ABSTRACT. The general properties of M giant and dwarf atmospheres are briefly reviewed, and the problems of modeling are described. We show, by means of recently calculated dwarf atmospheres, that molecules play a key role in the equation of state and that their absorption determines in most cases the slope of the spectrum. A comparison of calculated and observed spectra of the M-dwarf system Gliese 866 demonstrates the limitations of present modeling and the need for improved data on molecular equilibria and opacities.

Key words: OPACITIES – STARS: LATE-TYPE

1. INTRODUCTION

Most stars in the universe are M stars. More than 2/3 of the stars in the solar vicinity are M-type dwarfs. These inconspicuous objects at the lower end of the Main Sequence provide a substantial or even the dominant contribution to the mass of a galaxy. M-type giants and supergiants bear the crucial share of the integrated light in the red to the infrared portion of the spectrum of a galaxy. Still, detailed quantitative analyses of the spectra of M stars are rarely found in the literature, and the structure of their atmospheres is much less understood than that of most other spectral types.

Reliable M-dwarf model atmospheres provide access to the surface chemistry of a species of stars whose metallicity covers a range of four orders of magnitude. They also provide the boundary conditions needed for the construction of models for the interior, which is largely convective. With effective temperature, T_{eff}, and surface gravity, g, from spectral analysis, such models may yield the exact position in the HR diagram and the mass to luminosity ratio, M/L, of the lower Main Sequence.

M-type giants and supergiants comprise stars in the latest stages of stellar evolution feeding atmospheric material into interstellar space, and often showing admixtures of processed material in their atmospheres. Thus, accurate abundance analyses of these stars are crucial both for understanding the chemical evolution of a galaxy and for obtaining direct evidence of nuclear burning processes in stellar interiors.

If M-star atmospheres are so important beyond the general interest in interpreting a stellar

spectrum, then why does their modeling so much lag behind the rapid advances in modeling atmospheres of earlier spectral types during the past two decades?

M-star atmospheres cover an enormous range of gas pressures and temperatures not found in any other spectral type, resulting in an immense number of particle species to be considered in the equation of state and in summing up opacity contributions. Gas pressures in the uppermost photospheric layers of a late M-type Mira variable fall below 10^{-4} dyn/cm^2 and are even smaller in outer wind envelopes. At the bottom (typical optical depth $\tau = 10$) of the same atmosphere, one has about 10^3 dyn/cm^2, and gas pressures in M-dwarf atmospheres may be as high as 10^6 dyn/cm^2. Figs. 1 and 2 show typical gas pressures in static M-giant and M-dwarf photospheres. Kinetic temperatures range from below 1000 K in the surface layers of a cool Mira photosphere to, say, 7000 K around $\tau = 10$ in an early M-type giant. That is, they range from the conditions of occurrence of polyatomic molecules and dust particles to temperatures characteristic of the photosphere of the Sun. Consequently, M-star spectra exhibit a huge variety of molecular and atomic line spectra, whilst continuous absorption by H^- and H_2^- fades away towards lower temperatures owing to the lack of free electrons. The electron density in turn depends on the abundances of the alkali earth and alkali metals, which are less easily accessible to analyses than the iron-type metals supplying electrons in hotter stars.

The molecular line opacities depend sensitively not only on the element mixture of the atmosphere but also on T_{eff}, g, and the wavelength λ. Besides TiO, CN, CO and H_2O dominating the near-infrared region of an M-type spectrum, one finds various hydrides (CH, OH, MgH, SiH, CaH,...) and metal oxides (VO,...). In the latest spectral types, complex molecules, molecular clusters and dust grains occur. Except for the earliest and the most metal-depleted M stars, continuous absorption plays a role in very deep atmospheric layers only.

One of the most severe difficulties in constructing M-dwarf model atmospheres is the accurate and detailed treatment of convection. Apart from a tiny radiative equilibrium layer at the very surface, the atmospheric temperature stratification is determined by convective energy transport which, of course, cannot be treated in the adiabatic approximation in a stellar atmosphere. Any inaccuracy of the temperature at the transition point between radiative and convective layers propagates throughout the atmosphere and the stellar interior and may readily lead to erroneous results.

For low-mass, high-luminosity late M-type giants, the gas pressure scale height, H_p, around $\tau = 1$ in units of the stellar radius, R,

$$\frac{H_p}{R} \propto \frac{1}{T_{eff}} \frac{L^{1/2}}{M(g_{eff}/g)} \tag{1}$$

(g_{eff} = effective gravity) is not small compared to unity, which leads to a geometrically extended photosphere and various therewith connected modeling problems (cf. Baschek et al. 1991). Opacities react sensitively to the resulting geometrical cooling due to the dilution and peaking of radiation, the mutual amplification of geometrical cooling and of molecular cooling by H_2O absorption being a spectacular example. Non-static expanding outer envelopes and pulsating photospheres in which g_{eff} is a formally defined local quantity,

$$g_{eff} = -\frac{1}{\rho}\frac{dP}{dr} \tag{2}$$

(ρ = density, dP/dr = gas pressure gradient), have especially large H_p/R values values owing to small g_{eff}/g ratios. Moreover, the macroscopic velocity fields in these atmospheres result in depth-dependent line shifts affecting both the stratification through opacity effects and the spectra emitted at the surface. The pulsating (i.e. non-stationary) photospheres of Mira variables exhibit a particularly complicated velocity pattern (cf. Scholz 1992).

Since for M giants and supergiants an appreciable number of detailed model atmospheres and synthetic spectra have been published (cf. Gustafsson 1989), we will in the following focus our attention on molecular opacities in M-dwarf atmospheres for which few data are yet found in the literature. The discussion will mainly be based on the Ph.D. thesis of F. Allard in Heidelberg (1990). In Section 2 the chemical equilibria and the molecular absorption coefficients in these stars will be discussed by means of several examples. The consequences for the resulting energy distributions will be shown in the subsequent Section 3. We use the observations of Gl 866 to compare them with the calculated spectra (Section 4), and we conclude with a discussion of the need for further improvements.

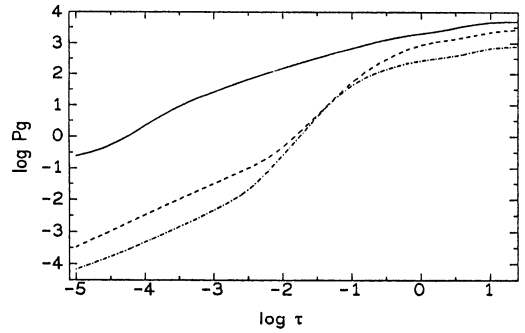

Fig. 1: The pressure distribution in the atmospheres of an AGB star with mass $M = 1\ M_\odot$, effective temperature $T_{eff} = 3500$ K and gravity $\log g = +0.72$ (——); of an AGB star with $M = 1M_\odot$, $T_{eff} = 3000$ K, $\log g = -0.01$ (– – –) and of a supergiant with $M = 15M_\odot$, $T_{eff} = 3000$ K, $\log g = -0.88$ (-.-.-.). For all objects solar composition is assumed.

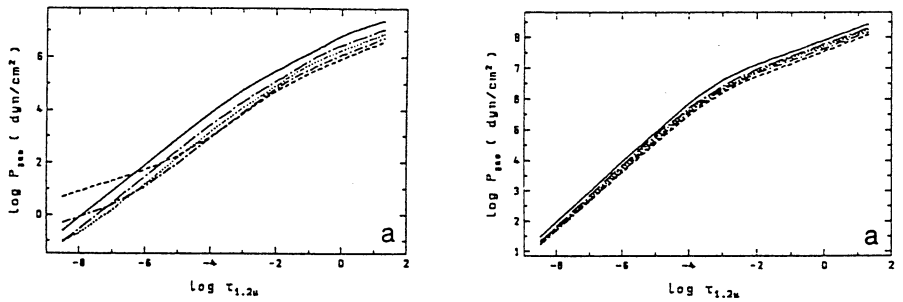

Fig. 2: Depth dependence of the gas pressure in M-dwarf atmospheres with $\log g = 5$ and $T_{eff} = 2000$ K (——), 2500 K (– . – .), 2750 K (.....), 3000 K (- . - . -) and 3500 K (- - - -). The left graph refers to solar composition, the right one to a metallicity $[M/H] = -3$.

2. CHEMICAL EQUILIBRIA AND ABSORPTION COEFFICIENTS IN M-DWARF ATMOSPHERES

In the equation of state a large number of species must be taken into account, since (i) the ranges of pressures and inverse temperatures $\Theta = 5040/T$—as mentioned above—are large, (ii) the electrons are often provided by rare elements with low ionization potential, (iii) the electron pressure results from a delicate equilibrium of these sources and the sinks of negative ions, (iv) quite a variety of species show up in the spectra and, finally, (v) several elements can be bound in various molecules so that the partial pressure of a species depends effectively on *many* equilibrium constants which in turn may have quite discrepant temperature and pressure dependences. Therefore up to 126 atomic and molecular species are considered in the calculations of Allard (1990). For given temperature, gas pressure and chemical composition all of them are first checked in an approximate calculation. When a species was found to be unimportant it was not taken into account in the final calculations so that the computing times could be significantly reduced.

As examples for typical M-dwarf results, we show in Fig. 3 the runs of the partial pressures of Mg^+ and 7 relevant molecules with optical depth for models with solar composition, gravity log g = 5 and effective temperatures of 2000, 2500, 2750, 3000 and 3250 K. The temperature distributions of these models (derived with the usual assumptions of hydrostatic equilibrium and depth independent flux of radiative plus convective energy) are given in Fig. 4. We see that the ionization degrees of metals like Mg are extremely low in the outer layers. Most of the electrons have to be supplied by atoms of very low ionization potential as Na, K and heavier alkali metals. Here even electrons generated by cosmic rays may play an important role.

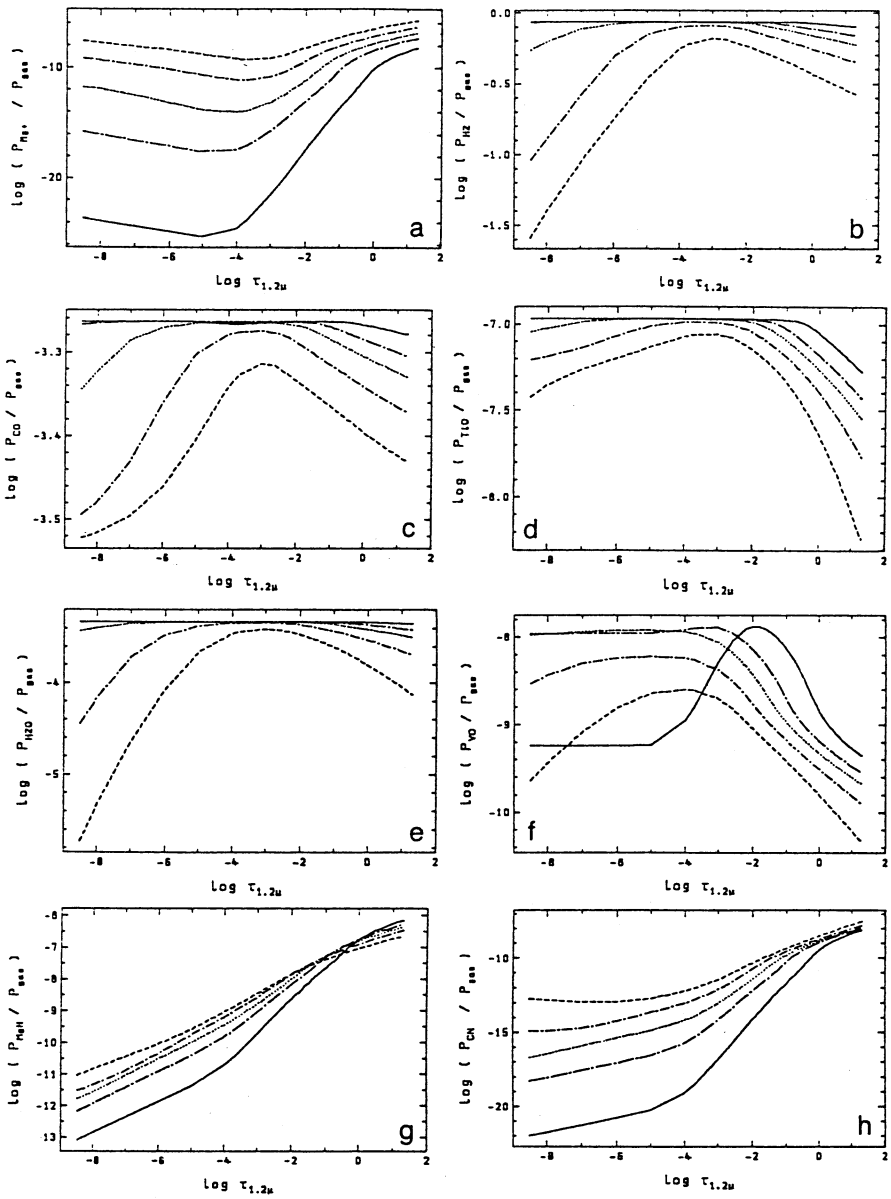

Fig. 3: Runs of the ratio of the partial pressures of Mg^+ and selected molecules to the total gas pressure with optical depth for M-dwarf models with $\log g = 5$ and solar composition. The curves refer to different effective temperatures, see Fig. 2.

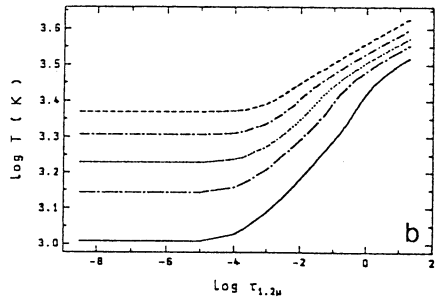

Fig. 4: Depth dependences of the temperature in M-dwarf atmospheres with solar composition and $\log g = 5$. The curves refer to different effective temperatures, see Fig. 2.

In the inner parts of the atmosphere, however, the temperatures are high enough so that significant fractions of Mg, Si and Fe are ionized. Note however that this behavior is partly due to the choice of $\tau_{1.2\mu}$ as abscissa since this optical depth is in turn largely determined by the electron pressure (see below). For the molecular partial pressures the only general rule seems to be that they decrease relative to the gas pressure in the very outer layers as a consequence of the steep decrease in the density at essentially constant temperature (cf. Figs. 1 and 4). Otherwise the curves reflect the complexity of the basic equations: in some cases the highest values are reached for the lowest temperatures, in others for the highest ones; sometimes the abundance of a molecule increases monotonically, and sometimes maxima are found; the absolute magnitudes of the fractional abundances may vary only by small factors, or they may vary by more than 10 orders of magnitude. It is evident that in the latter case it is virtually impossible to predict reliably the strengths of bands even if very accurate molecular data are available.

Some typical absorption coefficients that result from these equilibria are shown in Figs. 5 and 6. For the computation of the continuous coefficients we use the routines listed in Wehrse (1981), for H_2O the data of Ludwig (1971) are employed, and for the bands of diatomic molecules either straight mean values are taken from the literature or the cross-sections are calculated in the just-overlapping-line-approximation (JOLA). The latter approximations seem to be more reliable for M dwarfs than for giants because of pressure broadening due the high atmospheric densities. The required f-values are taken from various sources. Data from the laboratory or from *ab initio* calculations are in general preferred; however, in several cases they are not available or they seem to be quite uncertain so that we adopt values that give best fits for giants (Brett 1990).

The graphs show that for solar composition the main part of the spectrum is dominated by the bands of TiO and H_2O, in isolated spectral regions CO, VO, CaH, OH and other molecules show up. H^- is quite important, but H_2^- free-free absorption and the pressure induced H_2 opacities play only a minor role when the metallicity is high. The situation is quite different when the metallicity is reduced since most molecules become less abundant and therefore contribute less to the absorption whereas—as a consequence of the higher pressures—the pressure induced H_2 opacities get stronger. As a result, in the models of lowest metallicity these opacities are most important at all wavelengths of significant flux.

3. CALCULATED SPECTRA

Energy distributions that result from these absorption coefficients are shown in Figs. 7 to 9. The graphs demonstrate that for solar composition the molecular bands dominate completely the spectrum at all wavelengths, such that there are always strong deviations from the black body distribution and the continuum is hardly ever reached. When the metallicities are reduced the spectra get smoother first in the infrared range but for very low metal abundances also in the visible.

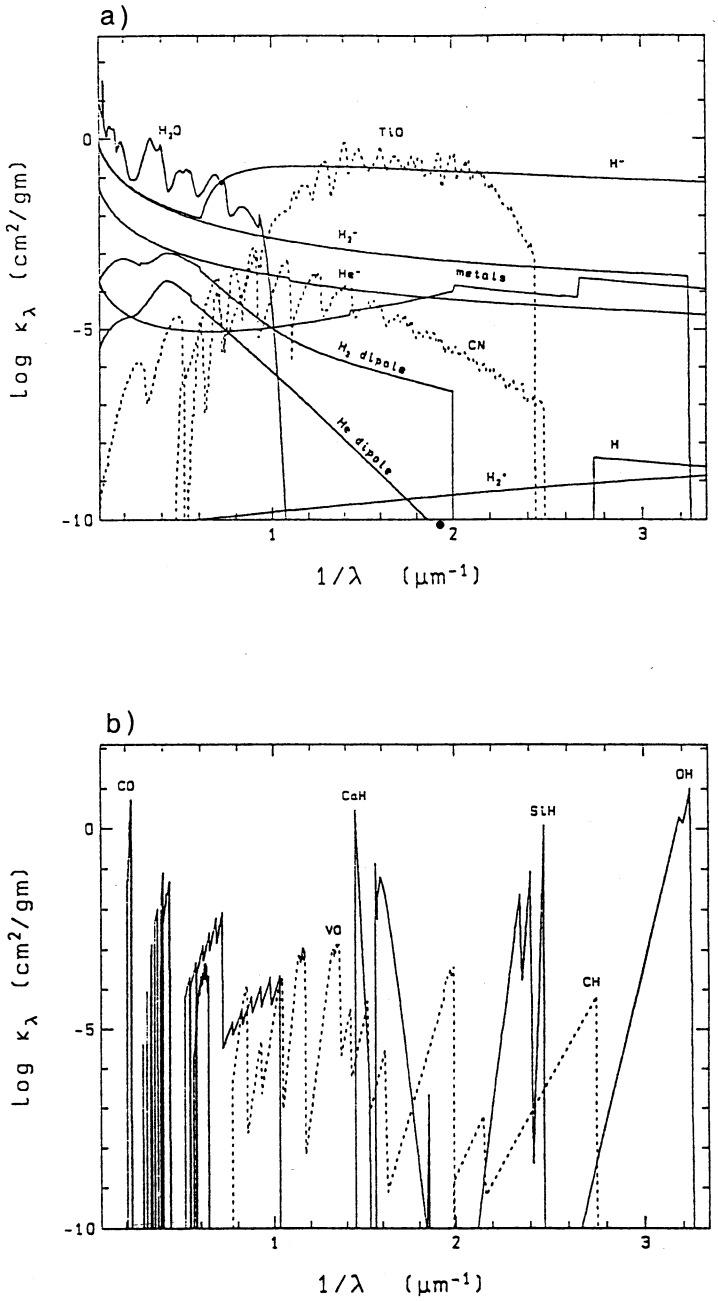

Fig. 5: Wavelength distribution of the absorption coefficients at optical depth $\tau_{1.2\mu} = 1$ in units of cm^2/g for a dwarf model with $T_{eff} = 3000$ K, $\log g = 5$, solar composition for a) the continuum sources (——) and the molecular bands of CN and TiO (- - -) and b) the molecular bands of the species taken into account in the just-overlapping line approximation (JOLA). The contributions by VO and CH are represented by broken lines for clarity.

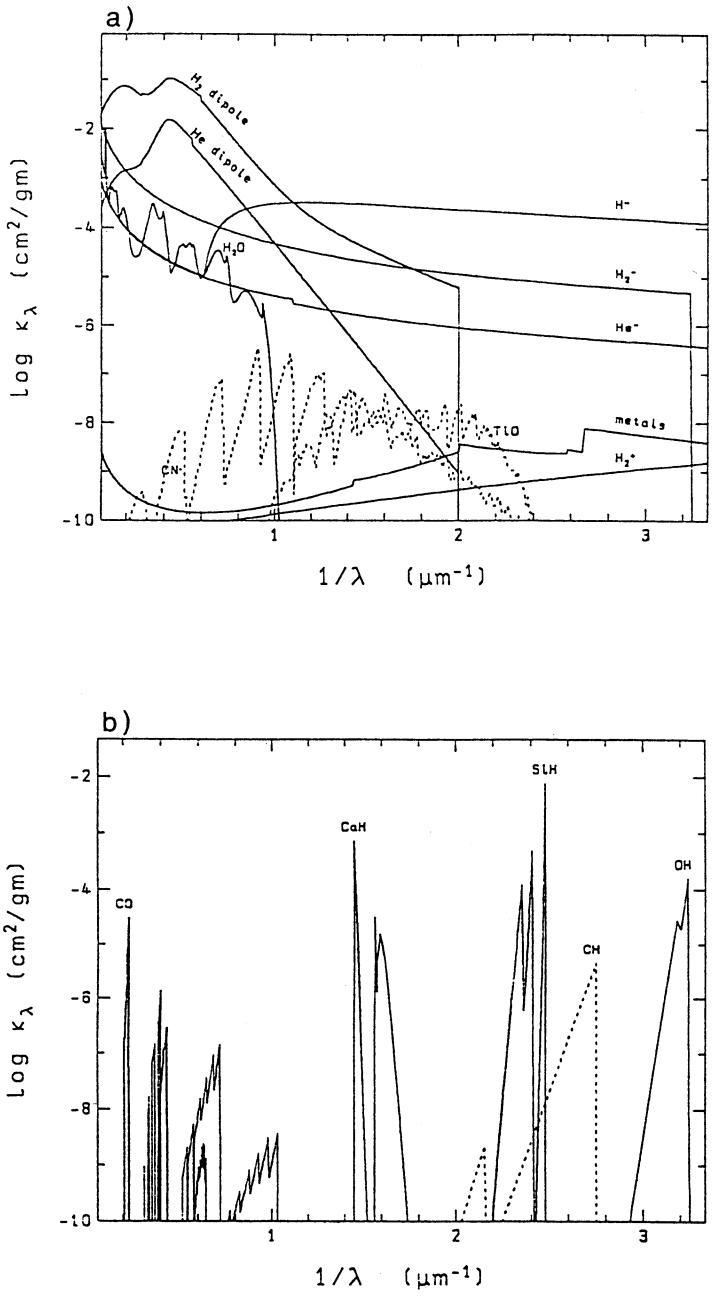

Fig. 6: Same as Fig. 5 but for a metallicity $[M/H] = -4$.

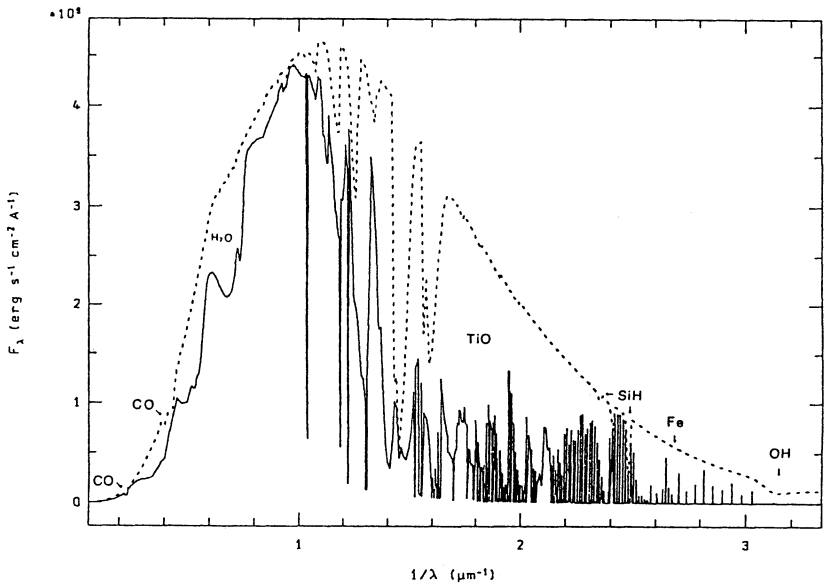

Fig. 7: Wavelength distribution of the flux emergent from a M-dwarf atmosphere with $T_{eff} = 3000$ K, $\log g = 5$ and solar composition. The full line gives the distribution when all absorbers are taken into account; in order to demonstrate the tremendous blocking in these atmospheres the energy distribution without the contributions of atomic lines, TiO and water-vapor bands is given by the dotted line for comparison. Some strong bands are indicated in addition.

4. COMPARISON OF THE CALCULATED SPECTRA WITH OBSERVATIONS

The degree to which synthetic spectra fit observed ones can be estimated for the relatively bright (V=14.2) and well studied system Gl 866 A+B (Leinert et al. 1990). The system consists of two close M dwarfs of similar effective temperatures so that it can essentially be modeled as one single object. Fig. 10 shows the comparison between the calculated energy distribution and fluxes obtained from color measurements from the near ultraviolet to the infrared range. In view of the large widths and of the uncertainties of the filter function the agreement seems to be acceptable; however, comparisons in color-color diagrams demonstrate that large uncertainties still exist not only when fluxes in the Wien part of the spectrum are involved but also for long wavelengths when steep gradients occur. The problems can best be seen from a comparison of low-resolution spectra in the visible range (Fig. 11): Most observed bands are present also in the models but their strengths are often quite discrepant. We attribute these differences mainly to errors in the electronic f-values and in the Franck-Condon factors, since the temperature gradient is essentially given by the adiabatic gradient and the pressures are so high that the assumed overlap of the rotational lines should not cause any problem. Note that the FeH band around 1 μm is not reproduced at all since for this molecule the spectroscopic data are not available, not even data of low accuracy. It should also be noted that for still cooler objects many (or even all) computed bands in the infrared range are in addition found to be much stronger than the observed ones (Bessell and Kui 1991). This might indicate that even the data for the computation of the adiabatic temperature gradient (e.g. data for the H_2 molecule) are not yet reliable for the temperatures and pressures in these objects.

When we go to high resolution the agreement may be better again, see for example Fig. 12, since only very few bands and atomic lines with good data may be involved. However, such spectra are difficult to obtain due to the intrinsic faintness of the M dwarfs and often not available (in particular for specific features of interest), but it seems that presently the parameters gravity and element abundances, which are derived from such spectra, are the least inaccurate ones.

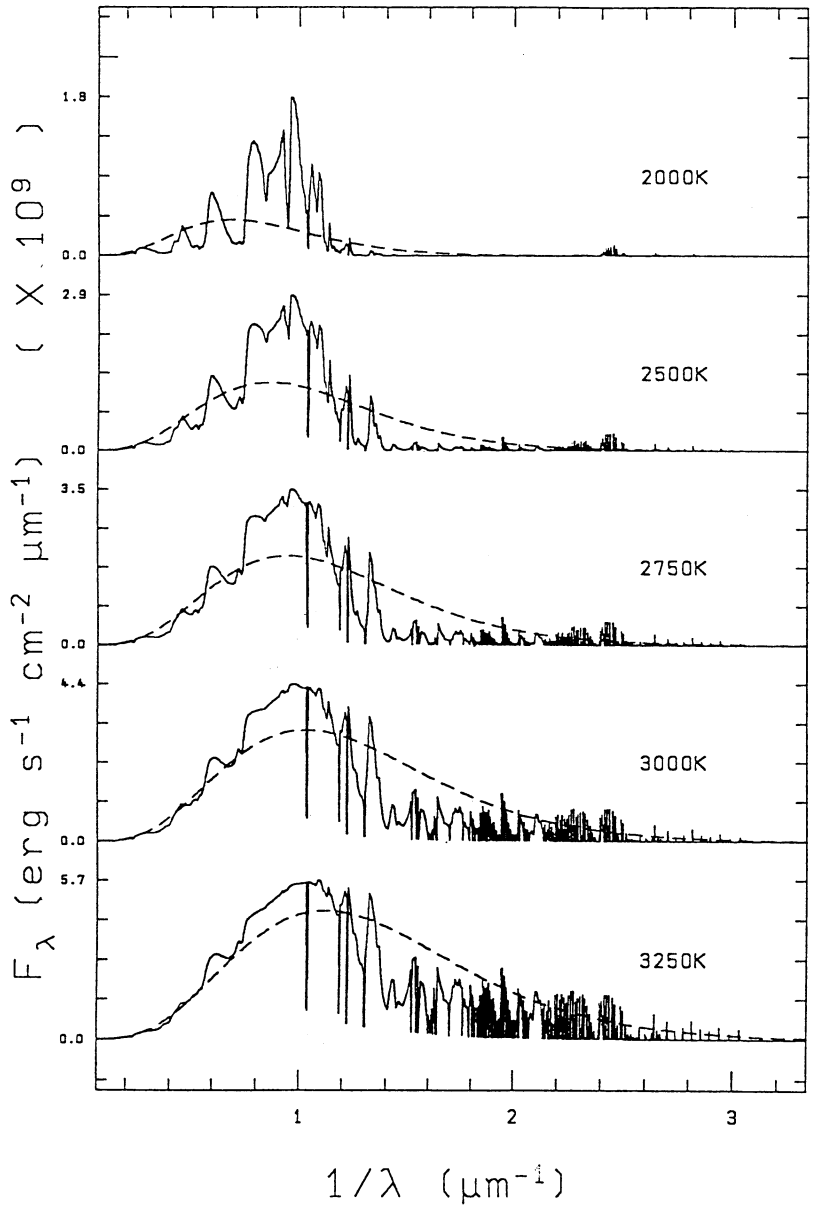

Fig. 8: Wavelength distribution of the emergent flux (full curves) for models with $\log g = 5$ and solar abundances. The effective temperatures range from 2000 K (upper panel) to 3250 K (lower panel). For comparison the black body distributions for the effective temperatures are shown by the broken curves.

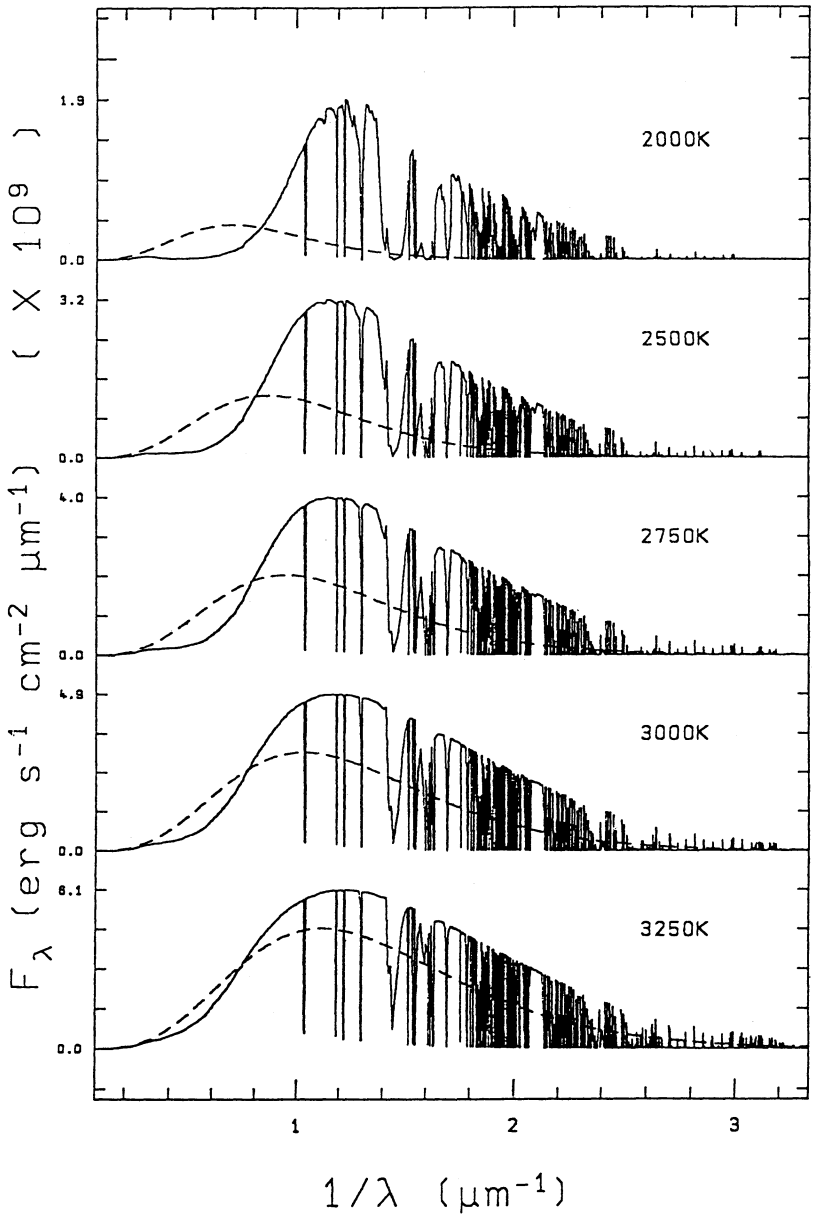

Fig. 9: Same as Fig. 8 but for metallicity $[M/H] = -3$.

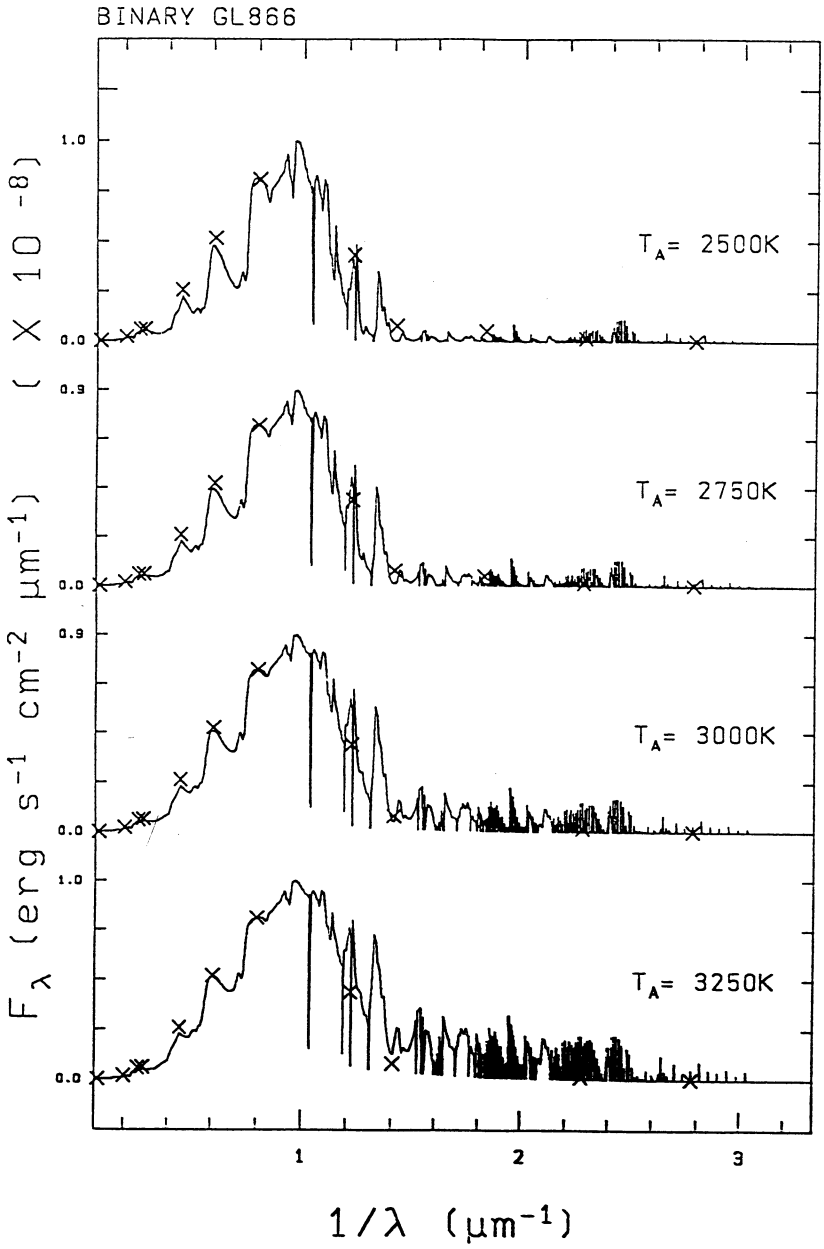

Fig. 10: Comparison of calculated energy distributions (full curves) with observed U, B, V, R, I, J, K, L, L' and M fluxes of the M-dwarf system Gliese 866. In all cases, solar composition and $\log g = 5$ are assumed. The effective temperature of the primary is indicated, that of the secondary M dwarf is estimated to be 2500 – 2750 K.

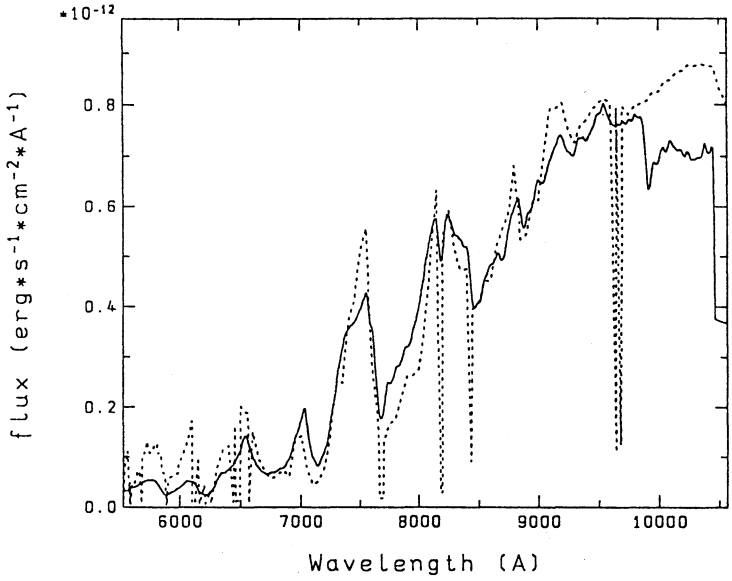

Fig. 11: Comparison of an observed low resolution spectrum of Gliese 866 (——) with the combined synthetic spectra of a 3000 K and a 2500 K dwarf star of solar composition and $\log g = 5$ (.....). The calculated spectrum has not been folded with the instrumental profile. Therefore the atomic lines appear too conspicuous. Otherwise, the comparison indicates the agreement that can be achieved with present data. Note in particular that the FeH band around 1μm is not reproduced at all due to the lack of data.

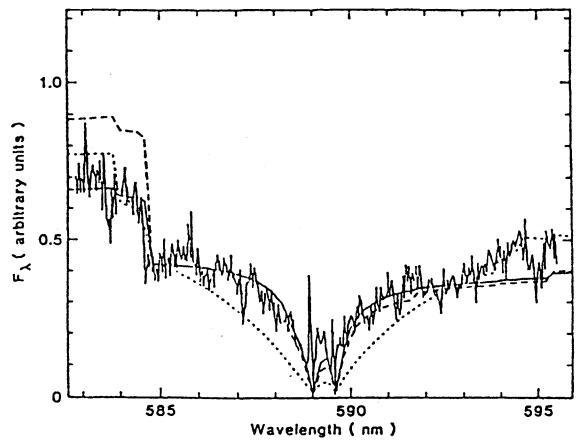

Fig. 12: Comparison of calculated and observed NaD profiles. The synthetic profiles refer to dwarfs with $T_{eff} = 3000$ K and solar composition (full curve), with $T_{eff} = 2750$ K and solar abundances (broken line) and with $T_{eff} = 3000$ K and reduced metallicity $[M/H] = -1$ (dotted curve). The "noise" in the observed spectrum is due to TiO bands, metal absorption lines and terrestrial features.

5. CONCLUSIONS

In conclusion, it must be stated that (i) the computational means (e.g. for handling very large sets of lines and complex equations of state, for treating complicated radiative transport, or for the determination of temperature distributions with extremely thin radiative layers) for constructing M-star model atmospheres and synthetic spectra are available; but that (ii) mainly due to the lack of reliable molecular data we cannot yet analyse the spectra of most of our neighbors in the Galaxy with a reliability that Unsöld reached in his analysis of the B0V star τ Sco half a century ago and that (iii) therefore one still has to concentrate on solar type or B, A, and F stars if accurate abundances are required (cf. Bessell and Scholz 1990)! This situation will only change when molecular opacities reach a similar accuracy to the atomic ones, the latter already available thanks to the activities of the Livermore group and the "Opacity Project".

Acknowledgement: We thank M. S. Bessell and J. Liebert for many stimulating discussions.

References:

Allard, F. 1990, Ph. D. thesis, University of Heidelberg
Baschek, B., Scholz, M., Wehrse, R. 1991, Astron. Astrophys. **246**, 374
Bessell, M.S., Kui, R. 1991, private communication
Bessell, M.S., Scholz, M. 1990, in: Accuracy of Element Abundances from Stellar Atmospheres, Wehrse, R., ed., Lecture Notes in Physics 356, Springer, p. 85
Brett, J. 1990, Astron. Astrophys. **231**, 440
Gustafsson, B. 1989, Ann. Rev. Astron. Astrophys. **27**, 701
Leinert, Ch., Haas, M., Allard, F., Wehrse, R., McCarthy, D.W., Jahreiß, H., Perrier, Ch. 1990, Astron. Astrophys. **236**, 399
Ludwig, C.B. 1971, Appl. Optics **10**, 1057
Scholz, M. 1992, Astron. Astrophys. **253**, 203
Wehrse, R. 1981, Monthly Notices Roy. Astron. Soc. **195**, 553

F. Allard: Department of Physics, University of Montreal, C.P. 6128, Succ. A, Montreal PQ H3C 3J7, Canada.
M. Scholz and R. Wehrse: Institut f. Theoret. Astrophysik der Universität Heidelberg, Im Neuenheimer Feld 561, W 6900 Heidelberg, Germany.